

# DEEP X-RAY LITHOGRAPHY FABRICATION OF mmWAVE CAVITIES AT THE ADVANCED PHOTON SOURCE\*

J.J. Song, Y.W. Kang, R.L. Kustom, A. Nassiri

Argonne National Laboratory, Argonne, IL 60439, USA

G. Caryotakis, E.N. Jongewaard, SLAC, Klystron Dept., Stanford, CA, USA

V. White, U. of Wisconsin at Madison, Center for X-ray Lithography, Madison, WI 53706, USA

## Abstract

Millimeter-wave (mmWave) accelerating cavity structures have been manufactured using the deep x-ray lithography (DXRL) technique. These cavity structures have potential applications as parts of linear accelerators, microwave undulators, and mm-wave amplifiers. The microfabrication process includes manufacturing of precision x-ray masks, exposure of positive resist by x-rays through the mask, resist development, and electroforming of the final microstructure. Prototypes of a 32-cell, 108-GHz constant-impedance cavity and a 66-cell, 94-GHz constant-gradient cavity were fabricated at APS. Using an HP8510C 26-GHz vector network analyzer, rf measurements are being prepared with a frequency up- and down-converter before and after a test cavity structure. Preliminary design parameters for a 91-GHz multi-module klystron along with an overview of the DXRL technology are also discussed.

## 1 INTRODUCTION

A potential advantage of mmWave accelerators for particle physics is a higher accelerating gradient. It is known from experience with S- or X-band accelerating structures that gradients are limited by dark current capture, which is the acceleration of field-emitted electrons to relativistic energies, and by rf breakdown. The maximum gradient from these phenomena scales approximately inversely with wavelength; scaling accelerating structures to significantly higher frequencies could provide a higher field gradient as proposed by P.B. Wilson [1].

The new micromachining technology, known as LIGA, consists of deep-etched x-ray lithography (DXRL), electroplating, and micromolding. The microfabrication processes have been developed by W. Ehrfeld and co-workers to the degree that submillimeter actuators, motors, and gears can be built with great accuracy and a high aspect ratio. Electric field levels as high as 50 MV/m and magnetic field levels of 1 T have been achieved with these components [2]. Specifically, this technology could offer significant advantages over conventional manufacturing methods in such areas as precision fabrication and mass production.

The concept of applying these techniques to develop

\*This work was supported by the U.S. Department of Energy, Office of Basic Energy Sciences, under Contract No W-31-109-ENG-38.

rf cavities for mm-wave linacs [3], undulators [4], free-electron lasers [5], and mm-wave amplifiers originated at Argonne National Laboratory. A meter-long structure with similar accuracy that also provides channels for vacuum pumping, adequate cooling, and focusing elements is feasible. Major challenges of the DXRL techniques are: fabrication of the wafers into three-dimensional rf structures, alignment and overlay accuracy of the structures, adhesion of the poly-methylmethacrylate (PMMA) on the copper substrate, and selection of a developer to obtain high resolution.

## 2 FABRICATION

The simplified version of the DXRL process is shown in Fig. 1. It consists of making an x-ray mask, preparing a sample and x-ray exposure, developing, and electroplating the structure. The process is related to the fabrication of semiconductor integrated circuits and requires similar tooling, in addition to a high-energy light source and electroplating equipment. In DXRL, no dissolution of unexposed positive thick resist is allowed during development, and good adhesion of the high-aspect ratio resist structure to the copper substrate is essential. In addition, the microstructures must have high mechanical stability and low internal stresses to prevent stress corrosion during exposure and development. Also, the resist material must be compatible with the electroplating process.

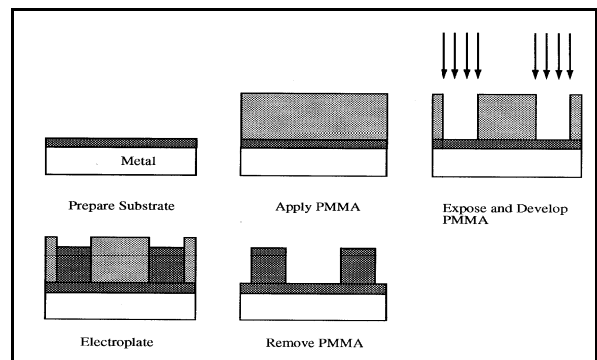


Figure 1: Simplified DXRL process.

DXRL with high-energy synchrotron radiation allows resists up to 1 mm thick to be fabricated with submicron accuracy. A high-accuracy DXRL mask was made by means of an intermediate mask--that is in two steps. The first step was the photolithography. A plating base of Ti/Au 75/300 Å was used for the e-beam writer and then a

3- $\mu\text{m}$ -thick layer of Au was plated on the intermediate mask. The second step used soft x-ray lithography at the Center for X-ray Lithography in Stoughton, Wisconsin (1-GeV Aladdin). For the DXRL mask, a 45- $\mu\text{m}$ -thick layer of Au was plated over a 300- $\mu\text{m}$ -thick Si wafer where the x-ray was exposed and the resist removed. To observe the high depth-to-width aspect ratio in the final product, micron-range structures were patterned on the DXRL mask. To avoid alignment problems and x-ray diffraction, these two steps were done on the same sample substrate without a physical gap.

PMMA up to 1 mm thick was used as a positive resist. The copper substrate was diamond-finished to have a flatness of 1  $\mu\text{m}$  over 4 inches. Then either an oxide film was grown to one micron thick or an equally thick Ti coating was deposited in order to promote better adhesion to the copper substrate. Through these processes, the flatness of the copper surface is maintained, but is still rough enough to give good adhesion to the PMMA sheet, which has a roughness of less than 0.1  $\mu\text{m}$  [6].

When the PMMA film was cast onto the copper substrate, it was annealed at various temperatures from 110 to 170° C for one to three hours [7]. The APS 2-BM-A beamline was used to expose the sample. The transmitted x-ray intensity was calculated based on the APS bending magnet parameters and is plotted in Fig. 2. The ratio of the top dose to the bottom dose for the 1-mm-thick PMMA is about 1.1. During the exposure, the sample was enclosed in a He-purged housing with a Kapton window, and the sample holder baseplate was water cooled. The first platinum (Pt) mirror with a grazing angle of 0.15° was used to cut off all the high-energy x-rays above 40 keV as shown in Fig. 2. More information on the APS 2-BM beamline for the DXRL can be found in Ref. 8.

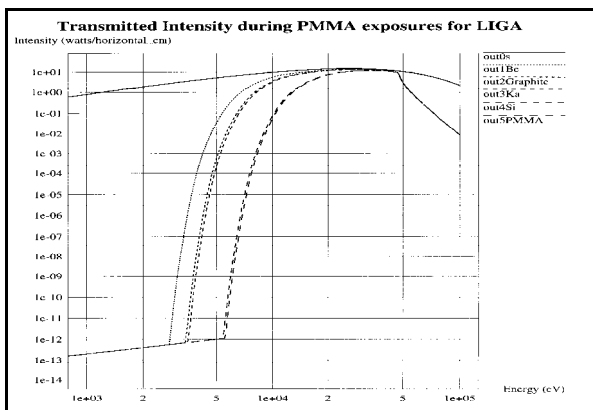


Figure 2: Transmitted x-ray intensity during PMMA exposures for DXRL at APS, energy vs. intensity.

Two different developers were used in the developing process. The first developer, so-called GG, was a mixture of 60% vol 2-(2-butoxy-ethoxy) ethanol, 20% tetrahydro-1, 4-oxazine, 5% 2-aminoethanol-1, and 15% deionized water. The allowed dose range was from 3 to about 10

$\text{kJ}/\text{cm}^3$ . Below that threshold the crosslinked resist could not be dissolved, and above that range damage to the resist can occur from production of gases in the PMMA. The second developer was methyl-iso-butyl ketone (MIBK) diluted with 2-propanol. After developing the microstructure, copper can be electroplated to the positive resist and the surface can be diamond-finished.

### 3 MM-WAVE STRUCTURES

Due to DXRL's ability to maintain precise tolerances, it is ideally suited for the manufacture of rf components operating at frequencies above 30 GHz. The first two structures fabricated were a 32-cell, 108-GHz constant-impedance cavity and a 66-cell, 94-GHz constant-gradient cavity. A 32-cell, 108-GHz constant-impedance cavity is a planar accelerating structure with parameters as shown in Table 1. The change from a typical cylindrical symmetrical disk-like structure to a planar accelerating structure results in a loss in shunt impedance and Q value of less than 5%. An accelerating gradient of 50 MV/m is chosen for a practical 50-MeV microlinac application, but it is not limited to 50 MV/m when the rf system is operational in the pulse mode with less repetition rate.

Table 1: The Design rf Parameters of a 32-Cell, 108-GHz Constant-Impedance Cavity

Frequency	f	108 GHz
Shunt impedance	R	312 $\text{M}\Omega/\text{m}$
Quality factor	Q	2160
Operating mode	TW	$2\pi/3$
Group velocity	$v_g$	0.043c
Attenuation factor	$\alpha$	13.5 $\text{m}^{-1}$
Accelerating gradient	E	50 MV/m
Peak power	P	750 kW

For a constant-impedance planar structure, the double-periodic structures with confluence in the p-mode design were considered. The  $2\pi/3$ -mode operation in these structures can give high shunt impedance, group velocity, and low sensitivity on dimensional errors. More detailed descriptions, such as rf simulation using the MAFIA computer code and the thermal analysis related to this structure, can be found in Ref. 9.

Constant-gradient accelerating structures are used in many present-day accelerators because of their higher energy gain and better frequency characteristics, such as higher shunt impedance, more uniform power dissipation, and lower sensitive to frequency deviations, when compared to the constant-impedance structure. Tapering the cells along the structure while keeping the gap and cell depth constant is difficult. Since the structure needs to be manufactured on a planar wafer, adjusting the cell width and length while maintaining a constant depth within the structure is necessary. Figure 3 shows the constant-gradient structure with cuts in the irises; its rf parameters can be found in Ref. 10.

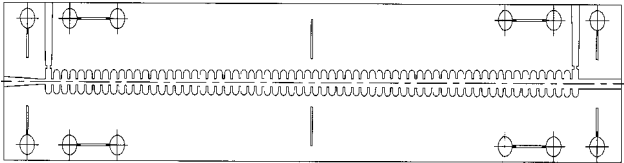


Figure 3: The 66-cell, 94-GHz constant-gradient cavity: side-coupling for mm-wave transmission and circled hole for the alignment.

#### 4 KLYSTRON DESIGN

The mm-wave amplifier is designed to meet a pulsed klystron operating at a high voltage, high current, by combing multi-cells and multi-modules as shown Figure 4 [11]. Beam optics become easier and permanent periodic magnet (PPM) focusing is possible. A higher efficiency also results, because of the low beam perveance. A number of klystrons can then be fabricated on a single substrate, using a deep-etch lithography technique. They can be water-cooled individually and operated in parallel. Several such modules can be stacked to form a klystron “brick,” requiring a relatively low voltage for the peak and average power produced. The brick can be provided with a single output, or with individual, spatially combined radiators. The klystron consists of a 4×10×1.5-inch module producing 500 kW peak, 500 W average at 91 GHz, operating at 120 kV, 10 A in total. Its main parameters are summarized in Table 2.

Table 2: Detailed Klystron Design Parameters

Frequency	91 GHz
Voltage	120 kV
Current	2.5 A
Perveance	$0.06 \times 10^{-6}$
Output power	125 kW
Pulse length	1 $\mu$ s
Drift tube diameter	0.8 mm
Beam diameter	0.5 mm
Cavity gap length	0.4 mm
Brillouin field	2.7 kG
Cathode current density	15 A/cm <sup>2</sup>
Magnetic period	6 mm
Duty cycle	0.1%
Beam area convergence	85:1

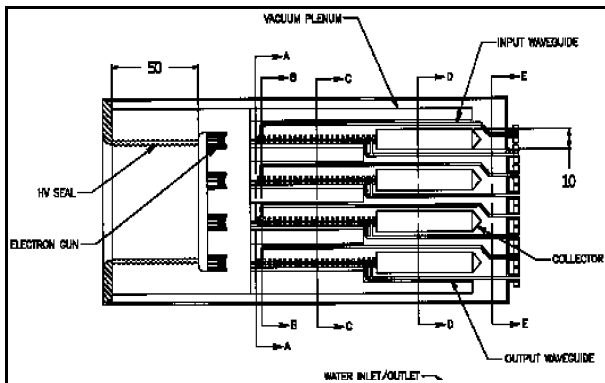


Figure 4: Four-klystron module layout.

The cathode loading and beam convergence parameters are quite conservative, except for the low perveance and PPM focusing. The beam voltage is very high for the power produced by a single klystron due to the low perveance required for PPM focusing (and for good efficiency). However, it is the PPM-focusing feature that makes the module design and tube paralleling possible.

#### 5 SUMMARY AND FURTHER WORK

The final electroplated structure for the prototype of the 108-GHz constant-impedance cavity is shown in Fig. 5. The size of the cavity cell appears to be a few microns off from the design, but the size is controllable by adjusting the x-ray mask to meet the specification. The roughness and flatness of the sidewall of the cavity cell were measured to be 0.05  $\mu$ m and 2  $\mu$ m, respectively.

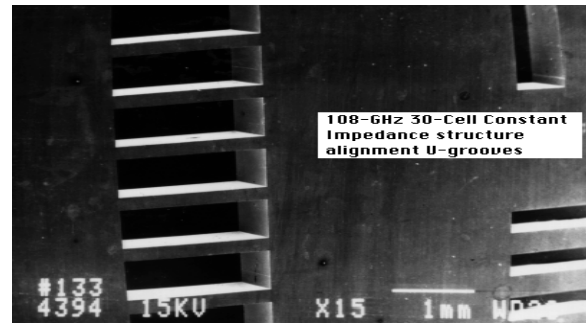


Figure 5: Scanning electron microscopy picture of the 108-GHz constant-impedance cavity structure.

Two mirror-imaged fabricated structures were aligned and measured on a network analyzer. The initial measurement of the quality factor is about 800, which is only 40% of the calculated value. The main contribution to the low value of Q is the MIBK chemical processing used to make the sample above. When the GG chemical was applied to develop the sample, the contrast between the exposed area and unexposed area was at least one order of magnitude higher than MIBK. The metallurgical study of the copper-electroplated sample shows that the level of oxygen in the sample appears to be too high. The electroplating process must be improved so that the structure can sustain against the vacuum and high-power rf.

#### REFERENCES

- [1] P.B. Wilson, SLAC-PUB-7263, Oct. 1996.
- [2] W. Ehrfeld and D. Muechmeyer, Nucl. Instr. and Methods in Physics Res., A203, 523 (1991).
- [3] Y.W. Kang et al., Proc. of the 1993 Particle Accelerator Conference, 549 (1993).
- [4] J.J. Song et al., SPIE-Micromachining and Microfabrication '96, Austin Texas, V2888 (1996).
- [5] A. Nassiri et al., IEEE, International Electron Device Conference, Washington DC, 169 (1993).
- [6] F. DeCarlo et al., submitted to 42nd International Conf. on Electron, Ion, and Photon Beam Tech '98, Chicago (1988).
- [7] H. Guckel et al., MEMS'91, Nara, Japan, January, 1991.
- [8] B. Lai et al., SPIE-Micromachining and Microfabrication '96, Austin Texas, V2888 (1996).
- [9] P. Matthews, and A. Khounsary, private communication.
- [10] J.J. Song et al., presented to HARMST'97, to be published in Microsystem Technologies.
- [11] G. Caryotakis et al., SPIE-Conf. of International Society of Optical Engineering '97, San Diego, CA.